Structure of Thermolysin Cleaved Microcin J25: Extreme Stability of a Two-Chain Antimicrobial Peptide Devoid of Covalent Links[†,‡]

K. Johan Rosengren,[§] Alain Blond,[+] Carlos Afonso,[#] Jean-Claude Tabet,[#] Sylvie Rebuffat,[+] and David J. Craik*[,§]

Institute for Molecular Bioscience, University of Queensland, Brisbane, QLD 4072, Australia, Laboratory of Chemistry and Biochemistry of Natural Substances, Department of Regulation, Development and Molecular Diversity, National Museum of Natural History, Paris, France, and Laboratory of Organic and Biological Structural Chemistry, UMR 7613 CNRS, University P. and M. Curie, Paris, France

Received November 26, 2003; Revised Manuscript Received February 12, 2004

ABSTRACT: The structure of a two-chain peptide formed by the treatment of the potent antimicrobial peptide microcin J25 (MccJ25) with thermolysin has been characterized by NMR spectroscopy and mass spectrometry. The native peptide is 21 amino acids in size and has the remarkable structural feature of a ring formed by linkage of the side chain of Glu8 to the N-terminus that is threaded by the C-terminal tail of the peptide. Thermolysin cleaves the peptide at the Phe10−Val11 amide bond, but the threading of the C-terminus through the N-terminal ring is so tight that the resultant two chains remain associated both in the solution and in the gas phases. The three-dimensional structure of the thermolysin-cleaved peptide derived using NMR spectroscopy and simulated annealing calculations has a well-defined core that comprises the N-terminal ring and the threading C-terminal tail. In contrast to the well-defined core, the newly formed termini at residues Phe10 and Val11 are disordered in solution. The C-terminal tail is associated to the ring both by hydrogen bonds stabilizing a short β-sheet and by hydrophobic interactions. Moreover, unthreading of the tail through the ring is prevented by the bulky side chains of Phe19 and Tyr20, which flank the octapeptide ring. This noncovalent two-peptide complex that has a remarkable stability in solution and in highly denaturing conditions and that survives in the gas phase is the first example of such a two-chain peptide lacking disulfide or interchain covalent bonds.

Microcin J25 (MccJ25)[1] is a small antimicrobial peptide belonging to the microcin family of ribosomally synthesized defense molecules secreted by *Enterobacteriaceae* and mediating microbial competition (*1*). It has generated widespread interest recently not only because of its high potency and intriguing structural characteristics but also because of its unusual mode of antibacterial action. Although most antimicrobial peptides are characterized by a large number of positive charges and are generally considered to interact with bacterial membrane structures (*2*), MccJ25 contains only a single positive charge and has been shown to inhibit bacterial transcription by interacting with the β' subunit of the *Escherichia coli* RNA polymerase (*3*, *4*).

Although originally isolated in 1992 from *E. coli* AY25 (*5*), it was not until 1999 that MccJ25 was characterized in more detail (*6*). At this point, it was proposed that the peptide consists of 21 amino acids arranged in a macrocyclic structure involving a peptide bond between the N- and the C-terminus. This suggestion was made on the basis of a range of biochemical techniques, including amino acid composition, mass spectrometry, NMR spectroscopy, and chemical and enzymatic degradation studies (*6*). Such a structure was consistent with the observations that neither of the termini were accessible for amino acid sequencing, the mass was consistent with a single posttranslational condensation reaction (i.e., loss of 18 mass units relative to a linear peptide), and further, digestion with thermolysin, which cleaved the peptide chain between Phe10 and Val11, resulted in a single product with a mass corresponding to a linear peptide. Subsequently, the solution structure of both native MccJ25 and a thermolysin-cleaved analogue (t-MccJ25) was determined, and it was shown that a macrocyclic structure was largely consistent with the structural information deduced by NMR (*7*, *8*). Several other naturally occurring antibacterial peptides with a macrocyclic backbone are known (*9*, *10*), and synthetic examples have been prepared recently (*11*, *12*).

However, recently we and two other independent research teams analyzed MccJ25 in more detail and concluded that the original NMR structure was incorrect. We concluded that in fact MccJ25 is not a macrocyclic peptide but comprises an unusual N-terminus to Glu8 side chain amide bond resulting in a N-terminal ring structure (*13*−*15*). Further, the C-terminal tail threads through the ring thus forming a noose-like feature. From this structure, it is clear that the positioning of two aromatic side chains in the C-terminal tail on each side of the ring results in the tail being trapped,

[†] D.J.C. is an Australian Research Council (ARC) professorial fellow. This work was in part funded by the ARC.

[‡] PDB accession number: 1S7P.

* Author to which correspondence should be addressed. Fax: +61-7-3346-2029. Phone: +61-7-3346-2019. E-mail: d.craik@imb.uq.edu.au.

[§] University of Queensland.

[+] National Museum of Natural History.

[#] University P. and M. Curie.

[1] Abbreviations: MccJ25, microcin J25; t-MccJ25, thermolysin cleaved MccJ25; RP-HPLC, reverse phase-high performance liquid chromatography.

10.1021/bi0361261 CCC: $27.50
Published on Web 03/27/2004

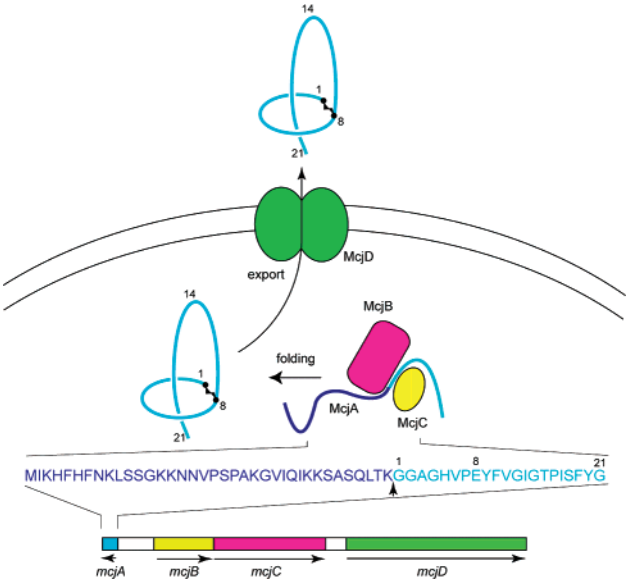

FIGURE 1: Schematic illustration of the production of MccJ25. The MccJ25 gene cluster, which is located on the pTUC100 plasmid, comprises four genes: mcjA (blue), mcjB (yellow), mcjC (pink), and mcjD (green). These encode the MccJ25 precursor (McJA), two processing/folding enzymes (McjB and McjC), and an exporter protein (McjD). The latter is involved in the secretion mechanism and is presumably also crucial for the self-immunity of the producing strain.

thus preventing unfolding of the molecule (*13*−*15*). This structure provides an explanation for all biochemical data reported on the peptide, and it is clear that it is the threaded arrangement that is responsible for the remarkable stability of MccJ25. Interestingly, the structure shares significant similarities, including the presence of a central β-sheet region, to the suggested macrocyclic model, highlighting the difficulty of characterizing such a complex structure.

The gene structure of the MccJ25 encoding plasmid pTUC100 has revealed that MccJ25 is expressed as a 58 amino acid precursor (McJA), which is presumably processed by two auxiliary proteins (McJB and McJC) that have been found to be crucial for the production of the mature product (Figure 1) (*16*). A fourth protein (McJD) is encoded in the gene cluster, and the sequence homology of this peptide with ABC transporter proteins suggests that it is involved in the export of MccJ25 and thus important for the self-immunity of the producing strain (*16*).

In this paper, we report the revised structure of thermolysin cleaved MccJ25 (t-MccJ25) and demonstrate, based on NMR and mass spectrometry data, that there is a tight association between the N- and the C-terminal fragments despite the lack of cross-links. A recent paper reported a remarkable stability of this protein by subjecting it to highly denaturing conditions, including 8 M urea and temperatures of above 100 °C, but the interpretation was based on what is now known to be an incorrect structure (*8*). It is therefore important to revise the structure and relate these findings to the correct structure. Furthermore, we show here that the tight two-chain association in t-MccJ25, as well as in two products generated by partial hydrolysis of MccJ25 in strong acidic conditions, survives the solution−gas phase transition. To our knowledge, t-MccJ25 is the first example of a two-chain peptide that has such a remarkable stability both in solution in highly denaturing conditions and in the gas phase but lacks disulfide or other interchain covalent bonds.

MATERIALS AND METHODS

Protein Expression and Purification. MccJ25, t-MccJ25, and two acidic hydrolysis fragments (h18-MccJ25 and h16-MccJ25) were obtained and purified as described previously (*6*, *8*). Briefly, t-MccJ25 was prepared by thermolysin digestion of native MccJ25 (1 μmol of MccJ25 was incubated in 8 M urea at 46 °C for 30 min before digestion by 40 μg of thermolysin (Boehringer, Mannheim) in 1200 μL of NH_4HCO_3, 10 mM $CaCl_2$ for 60 min at 46 °C and pH 8). h18-MccJ25 and h16-MccJ25 were obtained by adding 12 M HCl to MccJ25 at 37 °C for 10 h. The three peptides were purified by RP-HPLC on an Inertsil ODS2 column (5 μm, 4.6 × 25 mm), either under isocratic elution (acetonitrile in 0.1% aqueous CF_3COOH pH 2; 31:69 v/v; 1 mL/min) for t-MccJ25 or by a two-step linear gradient (acetonitrile in 0.1% aqueous CF_3COOH pH 2; 5−35% of acetonitrile in 35 min, followed by 35−50% acetonitrile in 5 min) for h18-MccJ25 and h16-MccJ25. Finally, a t-MccJ25 derivative carrying one urea molecule at the N-terminus (u-t-MccJ25) was generated by submitting t-MccJ25 to strong denaturing conditions (8 M urea, 65 °C, 16 h) followed by purification on a C18 Sep-Pak cartridge (Waters France) to remove the denaturing agent, as described previously (*8*).

NMR Spectroscopy. A 6 mM sample of t-MccJ25 in 100% CD_3OH was used to acquire DQF−COSY, TOCSY (spin lock 120 ms), NOESY (50, 100, 150, 200, and 400 ms) and ^{1}H-^{13}C HSQC and HMBC spectra on a DMX600 spectrometer equipped with a triple resonance ^{1}H-^{13}C-^{15}N-gradient probehead and a temperature controller system (BCU-05 refrigeration and BVT 3000 control units). Amide proton exchange rates were measured on a normal isotopic sample that was dissolved in CD_3OD at 0 °C and analyzed at 0 °C for 2 h and at 20 °C over 3 days by acquiring 1-D-^{1}H and TOCSY spectra.

Structure Calculations. Distance restraints for the calculation of the solution structure of t-MccJ25 were derived from a NOESY spectrum recorded at 600 MHz with a mixing time of 100 ms. Cross-peaks were assigned and integrated in XEASY (*17*) and converted to distance restraints using CYANA (*18*). Preliminary structures calculated in CYANA were used to resolve ambiguities in assignments, and after an iterative process, a final set of 129 interresidual distance restraints, including 64 long and medium range distances, was obtained. Dihedral restraints for the backbone angle ϕ and the side chain angle χ1 were derived from $^3J_{HNH\alpha}$ coupling constants and $^3J_{H\alpha H\beta}$ coupling constants in combination with intraresidual HN−Hβ and Hα−Hβ NOE intensities, respectively (*19*). On the basis of this analysis, the following restraints were used: ϕ −120° ±40° for $^3J_{HNH\alpha}$ > 8 Hz (Tyr9, Phe10, Ser18, Phe19, and Tyr20); χ1 60° ±30° for two small $^3J_{H\alpha H\beta}$ coupling constants (Ser18 and Tyr20); and χ1−60° ±30° for one small and one large $^3J_{H\alpha H\beta}$ coupling constant together with a strong/weak HN−Hβ, respectively (His5). Additional ϕ angle restraints of −100° ±80° were used in cases where a positive ϕ angle could be excluded based on a strong sequential Hα_i−HN$_{i+1}$ NOE in relation to the intraresidual Hα_i–HN$_i$ NOE (Ala3, Phe11, Ile13, and Tyr20). Finally, 10 restraints were included

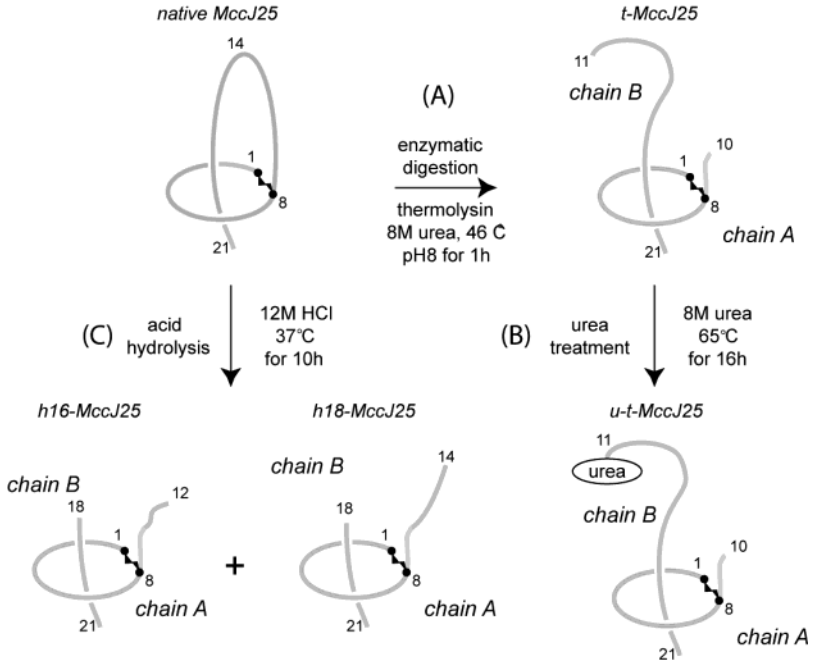

FIGURE 2: Generation of MccJ25 derivatives. (A) Digestion in vitro by thermolysin, resulting in a two-chain peptide with a break between Phe10 and Val11. (B) Treatment of the thermolysin digested peptide with 8 M urea at 65 °C leading to the coupling of a urea molecule to the N-terminus. (C) Hydrolysis of MccJ25 by 12 M HCl, resulting in several fragments, two of which are 18- and 16-residue two-chain peptides (h18-MccJ25 and h16-MccJ25).

for five hydrogen bonds (Gly2 HN → Phe19 O, Val6 HN → Tyr20 O, Glu8 HN → Ser18 O, Phe19 HN → Gly2 O, and Tyr20 HN → Val6 O) based on slow exchange behavior and close proximity to the acceptor in the preliminary structures. The final structural family was generated in CNS (*20*). This protocol involves torsion angle dynamics followed by refinement by Cartesian dynamics and Powell minimization in explicit solvent (*21*) as described previously (*22*).

Mass Spectrometry. The purified t-MccJ25, u-t-MccJ25, h18-MccJ25, and h16-MccJ25 were analyzed on a nanoESI-IT instrument (Esquire 3000, Bruker Daltonics) operating in the positive ion mode. Ion accumulation time was controlled by the ion charge control (ICC) system of the instrument (target 10 000). A potential of −650 V was applied on the counter electrode. Peptide samples (10 pmol/μL) were prepared in 50% MeOH/water with 0.5% formic acid. ITMS MS^n experiments were performed from selected ions (2 Da width) submitted to resonant excitation amplitude from 0.5 to 1.5 V_{P-P}. The recorded spectra are the average of 10−200 microscans to obtain a good signal-to-noise ratio. Two μL of each sample was loaded into Proxeon (Odense, Denmark) nanoelectrospray tips using Eppendorf GELoaders 1−10μL (Westbury, NY). The Roepstorff nomenclature (*23*) was used to describe peptide fragmentations.

RESULTS

Protein Expression and Purification. Four cleaved forms of the native antibacterial peptide MccJ25 were prepared and purified as shown in Figure 2. These were thermolysin cleaved MccJ25 (t-MccJ25), a derivative of t-MccJ25 carrying one urea molecule at the N-terminus (u-t-MccJ25), and two fragments of 18 and 16 residues (h18-MccJ25 and h16-MccJ25) that resulted from MccJ25 hydrolysis in strong acidic conditions and lacked residues T15-I17 and I13-I17, respectively (*6*). On the basis of the recently established structure of MccJ25 (*13*−*15*), these four peptides should contain two distinct peptide chains. The three-dimensional structure of t-MccJ25 was calculated, and IT-MS fragmentations of the four peptides were examined to analyze the stability in the gas phase of the noncovalent interactions involved in the two-chain structure.

NMR Spectroscopy and Spectral Assignment. Because of poor solubility in aqueous solvent and for comparison to the structural work recently published on native MccJ25, all NMR data for structural characterization were recorded in 100% d_3-MeOH at 600 MHz. The spectral data were of high quality, with generally sharp signals and minimal signal overlap. Resonance assignments were achieved using standard 2-D sequential assignment strategies and were identical to the assignments reported by Blond et al. (*8*). The two proline residues (Pro7 and Pro16) were both found to be in the trans conformation as evident from strong sequential $H\alpha_i-H\delta_{i+1}$ NOEs. For structure determination, distance restraints were derived from a NOESY spectrum recorded at 10 °C with a mixing time of 100 ms, and dihedral angle restraints were inferred from coupling constants measured from the splitting of amide signals either in the 1-D or a DQF−COSY spectra. From an analysis of chemical shifts, hydrogen/deuterium exchange, and the presence of medium- and long-range NOEs (Figure 3), it was clear that there is a tight association between the regions comprising residues 1−8 and residues 18−21. A general lack of medium-range NOEs is consistent with the absence of helical regions and tight turns, while several characteristic long-range NOEs, including a Hα−Hα connection between P7 and F19, indicate the presence of β-sheet structure. The complete lack of medium- and long-range NOEs in the residue 10−17 region, and the fact that the majority of the resonances originating from these residues show little deviation from

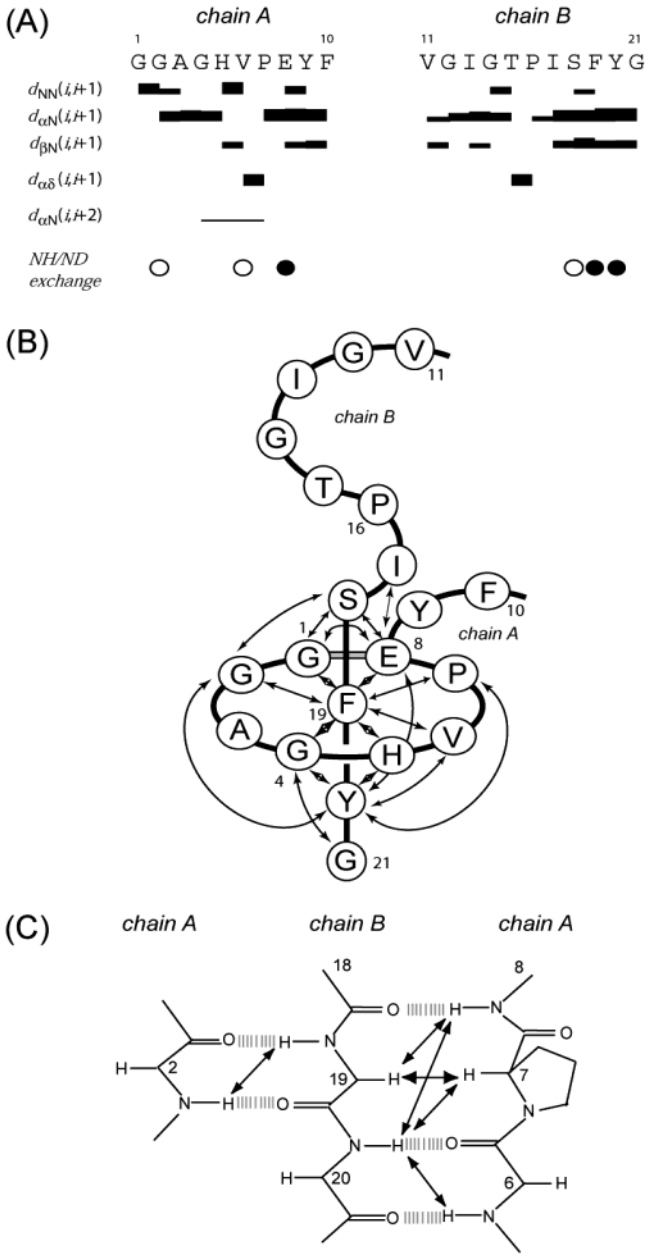

FIGURE 3: NMR data for t-MccJ25. (A) Barplot showing sequential and medium range NOE connectivities observed in the 100 ms NOESY spectrum of t-MccJ25. The thickness of the bars corresponds to the cross-peak intensity. The slow (1−2 days at 20 °C) and very slow (over 3 days at 20 °C) exchanging amide protons are indicated by white and black circles, respectively. (B) Schematic representation of the t-MccJ25 structure illustrating the long-range NOEs defining the threaded arrangement of the C-terminus. (C) Hydrogen bond interactions (broken lines) as deduced from amide exchange rates and structure calculations. Key backbone−backbone NOEs defining the β-sheet are indicated by arrows.

random coil chemical shifts, indicates that this region is likely to be flexible in solution.

Structure Determination and Analysis. The solution structure of t-MccJ25 was determined using simulated annealing by torsion angle dynamics followed by Cartesian dynamics and energy minimization in explicit solvent (*21*). Of a final family of 50 structures, the 20 lowest energy structures consistent with the experimental data were chosen to represent the solution structure of t-MccJ25 and this structural family is shown in Figure 4. These structures have no distance or angle violations of above 0.2 Å and 2°, respectively; furthermore, they have good covalent geometry as evident from minimal deviations from ideal bond lengths and angles.

It is clear that the structure has a well-defined core, which comprises the N-terminal octapeptide ring and the threading C-terminal fragment 18−21. The tail is tightly associated to the ring by the presence of both electrostatic interactions in the form of hydrogen bonding in a short β-sheet as well as hydrophobic interactions between the side chains of residues Val6, Pro7, and Phe19. In addition, there is a charge−charge interaction between the negatively charged C-terminus and the positively charged His5 side chain. The core is further stabilized by the presence of the bulky side chains of Phe19 and Tyr20. For the structure to unfold, the backbone segment associated with one of these side chains has to be threaded through the ring, which based on the tight fit, would seem impossible without the breaking of bonds. Apart from the structural core, it would appear, as suggested by NOE and chemical shift data, that the residue 11−17 region is highly flexible and disordered in solution.

Mass Spectrometry Analysis of the Stability of the Two-Chain t-MccJ25 in the Gas Phase. To examine the stability of the two-chain structure of t-MccJ25 in the gas phase, the CID patterns of both t-MccJ25 and u-t-MccJ25 on one hand, and the hydrolysis fragments h18-MccJ25 and h16-MccJ25 on the other hand, were analyzed and compared. At a relatively low declustering potential (i.e., low ion acceleration in the high pressure zone of the source), the MS spectra of the four peptides exhibited only MH^+ and $[M + 2H]^{2+}$ quasimolecular ions, indicating the presence of a single species (Figure 5A). MS^2 of either MH^+ (*m*/*z* 1813.9) (Figure 5B) or $[M + 2H]^{2+}$ (*m*/*z* 907.5) mainly resulted in a *b*-type ion series (*m*/*z* 1738.9, 1625.8, 1568.8, 1469.7, 1322.6, and 1159.6), which is consistent with the loss of G14-OH, I13, G12, V11, F10, and Y9, without the loss of the chain B (Figure 5C). A signal at *m*/*z* 1341.7 is observed at lower intensity, and this was concluded to result from the loss of the SFYG-OH peptide, based on further decomposition using an MS^3 experiment (data not shown). This occurred probably through the cleavage of a ring peptidic bond and is consistent with the loss of the chain B noncovalently bound to the ring.

The signal at *m*/*z* 1159.6, which corresponds to the ring that has lost the chain A tail but is still associated with the chain B is also observed in the MS spectrum recorded at a relatively high declustering potential (Figure 5A). The decomposition of this ion led to another *b*-type ion series at *m*/*z* 1084.6, 921.5, 774.4, and 687.4 (Figure 5D), indicative of the loss of G21-OH, Y20, F19, and S18 from chain B. MS^3 analysis of the *m*/*z* 687.4 ion, which corresponds to the ring, showed the loss of V6, H5, G4, A3, and G2, in agreement with a previous observation on t-MccJ25 by Wilson et al. (*15*) that the bond between V6 and P7 was broken, thus allowing the release of the chain B residues. Similar fragmentation patterns were observed for h16-MccJ25, t-MccJ25, and u-t-MccJ25. The series of *b*-ions in the chain A tail of h16-MccJ25 was, as expected, shifted to lower mass-to-charge ratios consistent with a mass loss of 170 Da, due to the absence of residues I13 and G14 in this peptide. Similarly, the fragmentation pattern of t-MccJ25 showed a competition between the loss of the chain B residues from G21 to V11 that are attached to the ring by noncovalent interactions and the short F10−Y9 segment

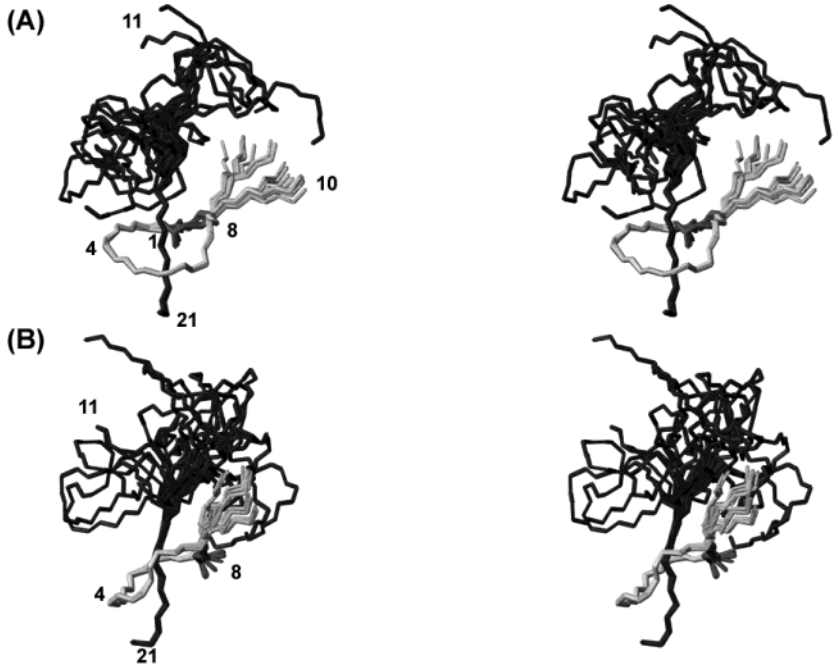

FIGURE 4: Stereoview of a family of 20 structures representing the solution structure of t-MccJ25. The structures are superimposed over residues 1−8 and 18−21. The N-terminal ring is shown in light gray, with the Gly1−Glu8 link in dark gray. As indicated by panel B, which is rotated 90° around the *y*-axis, the plane of N-terminal ring wraps around the C-terminus at an angle of approximately 45°.

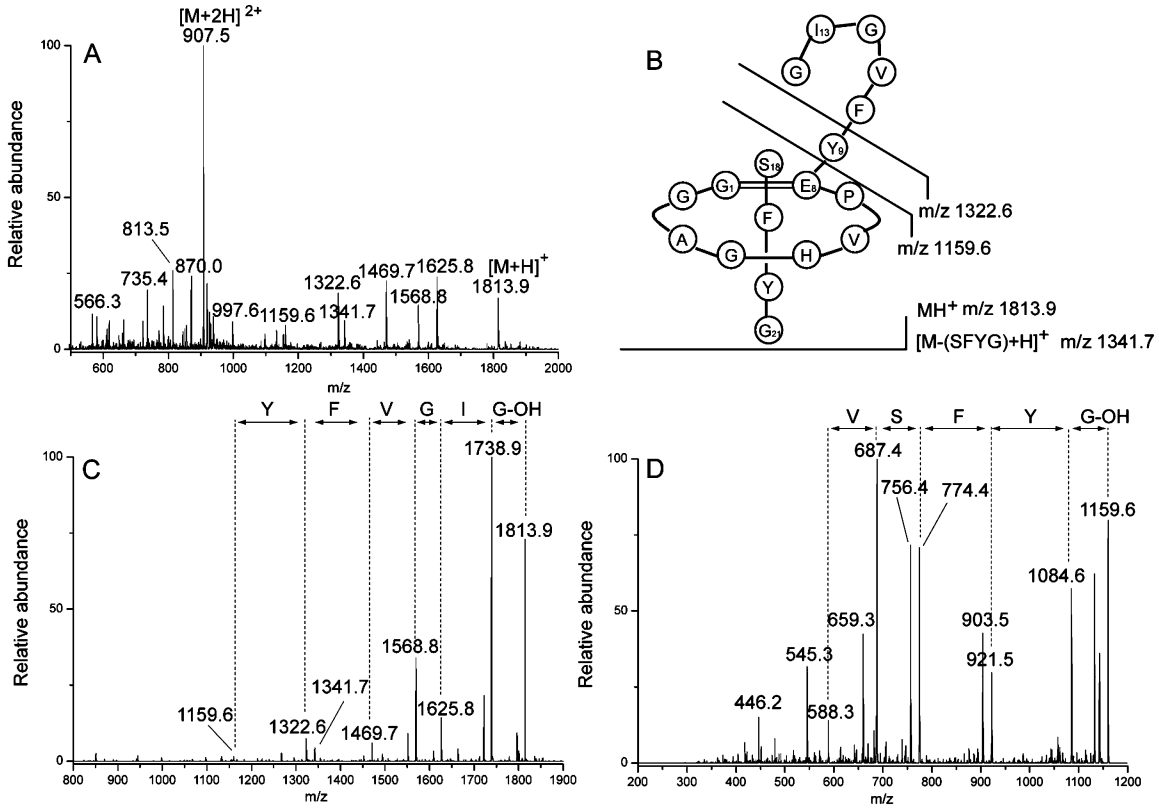

FIGURE 5: IT-MS data of h18-MccJ25, an 18-residue acidic hydrolysis fragment of MccJ25 containing the ring and six-residue tail in chain A and the four-residue chain B attached to chain A by noncovalent interactions. (A) MS spectrum showing the MH+ and [M + 2H]2+ species that characterize the presence of a single entity for this two-chain peptide, together with the major ions that were submitted to further decomposition. (B) Sequence and main fragment ions of h18-MccJ25. (C) MS^2 spectrum of the MH^+ ion at *m*/*z* 1813.9, showing the *b*-ion series indicative of the consecutive loss of G14-OH, I13, G12, V11, F10, and Y9 from chain A and the preservation of the noncovalently attached chain B. (C) MS^2 spectrum of the *m*/*z* 1159.6 ion showing losses of G21-OH, Y20, F19, and S18 from chain B followed by V6 from the ring.

covalently linked to the ring. In addition, u-t-MccJ25 exhibited the same chain B ion series as t-MccJ25 but shifted to higher mass-to-charge ratios consistent with an increase in mass of 43 Da, due to the presence of the urea molecule at the N-terminus, thus confirming the origin of these ions. Taken together, these data, which are in agreement with previous results on the thermolysin-digested MccJ25 (*15*), clearly show that the chain B fragment, while not linked to

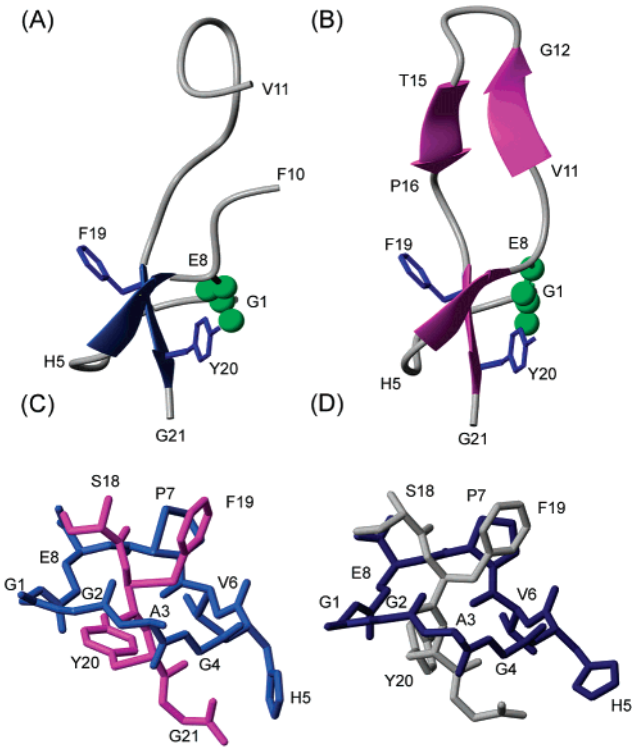

FIGURE 6: Comparison of t-MccJ25 (A and C) with native MccJ25 (B and D). The top panels show the lowest energy structures in ribbon style diagrams illustrating the elements of secondary structure. The bottom panels show the threaded arrangement and the retained structural core, illustrating the tight association between the N- and the C-terminal regions both in native and in t-MccJ25. The positioning of the aromatic side chains F19 and Y20 on each side of the ring prevents the unfolding of the structure.

the chain A by a covalent bond, is firmly attached to it whatever its size and that this noncovalent stabilization is preserved in the gas phase upon CID experiments.

DISCUSSION

In this paper, we have reported the structural characterization by NMR and MS of t-MccJ25, the product of thermolysin digestion of the antimicrobial peptide MccJ25. Recently, the structure of native MccJ25 was revised, demonstrating that it is not, like first believed, a macrocyclic peptide but comprises a noose-like structure characterized by an N-terminus to Glu8 side chain link and a threaded C-terminus (*13*−*15*). From our analysis of the thermolysin cleaved peptide, it is clear that this remarkable arrangement is extremely stable, and in fact, the two chains stay together as one entity after breakage of the loop between the ring and the threaded part of the C-terminus. This unique stability of the cleaved peptide makes it interesting to further investigate what structural features of native MccJ25 are retained after enzymatic digestion.

Figure 6 shows a comparison between native and t-MccJ25, and from this it is clear that the core regions, including the N-terminal ring and the threading C-terminal tail, are identical. In contrast, the β-hairpin region, which links the ring and the tail, is clearly disrupted in the cleaved peptide, and the result is a disordered region comprising residues 11−16. As predicted from the native structure, it appears that the bulky aromatic side chains of Phe19 and Tyr20 positioned on each side of the N-terminal ring play a crucial part in the stability of this peptide, as unfolding would require breakage of bonds to free the C-terminus. This is consistent with the remarkable findings of Blond et al. who reported that t-MccJ25 is not degraded by treatment by 8 M of urea at 65 °C for 16 h, a treatment that even allows coupling of one urea molecule to the peptide N-terminus, and furthermore, showed that temperatures of 165 °C were needed to irreversibly disrupt the structure (*8*). This two-chain structure observed in solution for t-MccJ25 is also maintained in strong acidic conditions, which result in the breaking of several covalent bonds, and the extraordinary noncovalently bound complex even survives in the gas phase at a relatively high declustering potential. The latter observation has also been reported for the structurally related peptide RES-701-1 by Loo et al., who showed that such peptides are examples in which the higher order structure of a gas phase ion relates directly to its solution phase structure (*24*). Such an unusual structural stability (i.e., a tail being tightly locked in a ring in such a manner that it cannot be extricated from it without breakage of covalent bonds) is due to a combination of noncovalent interactions and steric hindrance related to the orientation of Phe19 and Tyr20 bulky aromatic side chains as regard to the tight ring.

It has previously been shown that the thermolysin-cleaved MccJ25 retains some antimicrobial activity, although the efficacy is greatly reduced as compared to native (*8*). Native MccJ25 has the unique antibacterial action of inhibiting RNA polymerase but according to other reports also has the ability to disrupt membrane structures in some bacterial strains (*25*, *26*). Nothing is currently known about which regions of MccJ25 are responsible for the inhibition of RNA polymerase, but it seems likely that some of the residue 11−16 hairpin region is involved in this interaction, and the complete disruption of this structural element would thus affect the binding. At this point, it is difficult to speculate on whether the remaining activity is due to the fact that the structural core is retained and still has the ability to inhibit RNA polymerase or if it is a result of a disruption of membranes.

There are several examples of two-chain bioactive peptides with important functions. Among the most well-known is insulin, which is synthesized as a single chain peptide that is folded and oxidized to form three disulfide bonds. Subsequently, part of the chain is removed by proteolysis, which results in a bioactive product that comprises two peptide chains linked by two disulfide bonds and with a third intrachain disulfide bond (*27*). However, t-MccJ25 is fundamentally different from insulin in that it does not have a covalent cross-link between the chains and relies solely on the steric-link through which the C-terminal is locked in place in the N-terminal ring.

Recent development of bacterial resistance toward commonly used antibiotics has sparked a widespread interest in natural antibiotic substances as potential leads for novel drugs. MccJ25 is a remarkable peptide with high potency and proteolytic and thermal stability, which makes it interesting from a pharmaceutical viewpoint. The unique structure presents a significant challenge from the perspective of chemical synthesis. In vivo, the molecule relies on the help of two plasmid-encoded processing enzymes for folding and cross-linking, and it would clearly be difficult to achieve

this folding in vitro. Currently, mutational studies are being undertaken, and the results will provide additional information on both the folding process and the interaction with the chaperones as well as the mechanism of action and the inhibition of RNA polymerase. On the basis of the features of native MccJ25 and its thermolysin-cleaved analogue, such insights have the possibility to open the door for the design of novel antibiotic compounds mimicking the MccJ25 mode of action.

ACKNOWLEDGMENT

This work was supported in part by a grant (D.J.C.) from the Australian Research Council. We are pleased to thank Prof. D. Davoust for access to the NMR facilities in the NMR Laboratory at the University of Rouen and Christophe Goulard for technical assistance in preparing the peptides.

REFERENCES

1. Destoumieux-Garzon, D., Peduzzi, J., and Rebuffat, S. (2002) Focus on modified microcins: structural features and mechanisms of action, *Biochimie 84*, 511−9.
2. Epand, R. M., and Vogel, H. J. (1999) Diversity of antimicrobial peptides and their mechanisms of action, *Biochim. Biophys. Acta 1462*, 11−28.
3. Delgado, M. A., Rintoul, M. R., Farias, R. N., and Salomon, R. A. (2001) *Escherichia coli* RNA polymerase is the target of the cyclopeptide antibiotic microcin J25, *J. Bacteriol. 183*, 4543−50.
4. Yuzenkova, J., Delgado, M., Nechaev, S., Savalia, D., Epshtein, V., Artsimovitch, I., Mooney, R. A., Landick, R., Farias, R. N., Salomon, R., and Severinov, K. (2002) Mutations of bacterial RNA polymerase leading to resistance to microcin j25, *J. Biol. Chem. 277*, 50867−75.
5. Salomon, R. A., and Farias, R. N. (1992) Microcin 25, a novel antimicrobial peptide produced by *Escherichia coli*, *J. Bacteriol. 174*, 7428−35.
6. Blond, A., Peduzzi, J., Goulard, C., Chiuchiolo, M. J., Barthelemy, M., Prigent, Y., Salomon, R. A., Farias, R. N., Moreno, F., and Rebuffat, S. (1999) The cyclic structure of microcin J25, a 21-residue peptide antibiotic from *Escherichia coli*, *Eur. J. Biochem. 259*, 747−55.
7. Blond, A., Cheminant, M., Segalas-Milazzo, I., Peduzzi, J., Barthelemy, M., Goulard, C., Salomon, R., Moreno, F., Farias, R., and Rebuffat, S. (2001) Solution structure of microcin J25, the single macrocyclic antimicrobial peptide from *Escherichia coli*, *Eur. J. Biochem. 268*, 2124−33.
8. Blond, A., Cheminant, M., Destoumieux-Garzon, D., Segalas-Milazzo, I., Peduzzi, J., Goulard, C., and Rebuffat, S. (2002) Thermolysin-linearized microcin J25 retains the structured core of the native macrocyclic peptide and displays antimicrobial activity, *Eur. J. Biochem. 269*, 6212−22.
9. Craik, D. J., Daly, N. L., Saska, I., Trabi, M., and Rosengren, K. J. (2003) Structures of naturally occurring circular proteins from bacteria, *J. Bacteriol. 185*, 4011−4021.
10. Trabi, M., and Craik, D. J. (2002) Circular proteins—no end in sight, *Trends Biochem. Sci. 27*, 132−8.
11. Otvos, L., Jr., Bokonyi, K., Varga, I., Otvos, B. I., Hoffmann, R., Ertl, H. C., Wade, J. D., McManus, A. M., Craik, D. J., and Bulet, P. (2000) Insect peptides with improved protease-resistance protect mice against bacterial infection, *Protein Sci. 9*, 742−9.
12. Yu, Q., Lehrer, R. I., and Tam, J. P. (2000) Engineered salt-insensitive _-defensins with end-to-end circularized structures, *J. Biol. Chem. 275*, 3943−9.
13. Rosengren, K. J., Clark, R. J., Daly, N. L., Goransson, U., Jones, A., and Craik, D. J. (2003) Microcin J25 has a threaded side chain-to-backbone ring structure and not a head-to-tail cyclized backbone, *J. Am. Chem. Soc. 125*, 12464−74.
14. Bayro, M. J., Mukhopadhyay, J., Swapna, G. V., Huang, J. Y., Ma, L. C., Sineva, E., Dawson, P. E., Montelione, G. T., and Ebright, R. H. (2003) Structure of antibacterial peptide microcin J25: a 21-residue lariat protoknot, *J. Am. Chem. Soc. 125*, 12382−3.
15. Wilson, K. A., Kalkum, M., Ottesen, J., Yuzenkova, J., Chait, B. T., Landick, R., Muir, T., Severinov, K., and Darst, S. A. (2003) Structure of microcin J25, a peptide inhibitor of bacterial RNA polymerase, is a lassoed tail, *J. Am. Chem. Soc. 125*, 12475−83.
16. Solbiati, J. O., Ciaccio, M., Farias, R. N., Gonzalez-Pastor, J. E., Moreno, F., and Salomon, R. A. (1999) Sequence analysis of the four plasmid genes required to produce the circular peptide antibiotic microcin J25, *J. Bacteriol. 181*, 2659−62.
17. Eccles, C., Guntert, P., Billeter, M., and Wüthrich, K. (1991) Efficient analysis of protein 2-D NMR spectra using the software package EASY, *J. Biomol. NMR 1*, 111−30.
18. Herrmann, T., Guntert, P., and Wuthrich, K. (2002) Protein NMR structure determination with automated NOE assignment using the new software CANDID and the torsion angle dynamics algorithm DYANA, *J. Mol. Biol. 319*, 209−27.
19. Wagner, G., Braun, W., Havel, T. F., Schaumann, T., Go, N., and Wuthrich, K. (1987) Protein structures in solution by nuclear magnetic resonance and distance geometry. The polypeptide fold of the basic pancreatic trypsin inhibitor determined using two different algorithms, DISGEO and DISMAN, *J. Mol. Biol. 196*, 611−39.
20. Brunger, A. T., Adams, P. D., Clore, G. M., DeLano, W. L., Gros, P., Grosse-Kunstleve, R. W., Jiang, J. S., Kuszewski, J., Nilges, M., Pannu, N. S., Read, R. J., Rice, L. M., Simonson, T., and Warren, G. L. (1998) Crystallography and NMR system: A new software suite for macromolecular structure determination, *Acta Crystallogr. D54* (Pt 5), 905−21.
21. Linge, J. P., and Nilges, M. (1999) Influence of nonbonded parameters on the quality of NMR structures: a new force field for NMR structure calculation, *J. Biomol. NMR 13*, 51−9.
22. Rosengren, K. J., Wilson, D., Daly, N. L., Alewood, P. F., and Craik, D. J. (2002) Solution structures of the cis- and trans-Pro30 isomers of a novel 38-residue toxin from the venom of *Hadronyche infensa* sp. that contains a cystine-knot motif within its four disulfide bonds, *Biochemistry 41*, 3294−301.
23. Roepstorff, P., and Fohlman, J. (1984) Proposal for a common nomenclature for sequence ions in mass spectra of peptides, *Biomed. Mass Spectrom. 11*, 601.
24. Loo, J. A., He, J. X., and Cody, W. L. (1998) Higher order structure in the gas-phase reflect solution structure, *J. Am. Chem. Soc. 120*, 4542−3.
25. Rintoul, M. R., de Arcuri, B. F., and Morero, R. D. (2000) Effects of the antibiotic peptide microcin J25 on liposomes: role of acyl chain length and negatively charged phospholipid, *Biochim. Biophys. Acta 1509*, 65−72.
26. Rintoul, M. R., de Arcuri, B. F., Salomon, R. A., Farias, R. N., and Morero, R. D. (2001) The antibacterial action of microcin J25: evidence for disruption of cytoplasmic membrane energization in *Salmonella* newport, *FEMS Microbiol. Lett. 204*, 265−70.
27. Robinson, C. (1953) Structure of insulin, *Nature 172*, 773−4.

BI0361261